

UNDERSTANDING THE PWM NON-LINEARITY

Toit Mouton
6 March 2012

Understanding the PWM non-linearity

Inaugural lecture delivered on 6 March 2012

Prof H du T Mouton
Department of Electrical and Electronic Engineering
Faculty of Engineering

Editor: SU Language Centre
Printing: rsamprinters@gmail.com

ISBN: 978-0-7972-1344-9

Copyright © Stellenbosch University Language Centre



ABOUT THE AUTHOR

Hendrik du Toit Mouton was born in Somerset-West in 1965. In 1976 his family moved from Stellenbosch to Bloemfontein where he matriculated in 1983. He started his B.Sc. at the University of the Orange Free State in 1984 and majored in Mathematics and Physics. After completing a B.Sc.(Hons) and M.Sc. in Mathematics he was appointed as lecturer in Mathematics at the University of the Orange Free State in 1990. He completed his Ph.D. in Mathematics, on Fredholm theory relative to Banach Algebra homomorphisms, under the supervision of Prof. Heinrich Raubenheimer in 1991. During the second semester of 1992 he spent a six month sabbatical, during which time he collaborated with Prof. Sandy Grabiner from Pomona College in the USA and Prof. Bernard Aupetit from Laval University in Canada.

In 1995 he moved to Stellenbosch and enrolled for the degree Bachelor in Electrical and Electronic Engineering, which he received in 1996. In 1997 he enrolled for a Ph.D. in Electrical Engineering under the supervision of Prof. Johan Enslin on a high power converter for a superconducting magnet. He was appointed as senior lecturer in Power Electronics in October 1997 and completed his Ph.D. in Electrical Engineering in 2000. In 2001 he was promoted to associate professor in Power Electronics. In 2003 he spent a sabbatical at the University of Toulouse, where he collaborated with Dr Thierry Meynard, and the University of Wuppertal, where he collaborated with Prof. Ralph Kennel.

His research team collaborates closely with industry and generates the majority of its research funding through contract research for ESKOM. He currently collaborates on research projects with the Technical University of Munich, The Royal Melbourne Institute of Technology and Hypex Electronics in Groningen.

His research interests include high power converters, multilevel converters, modulation theory and class-D audio amplifiers.

UNDERSTANDING THE PWM NON-LINEARITY

I. INTRODUCTION

Fixed frequency pulse-width modulation (PWM) forms the basis for controlling a vast variety of power electronic converters. The applications of pulse-width modulation range from simple buck converters to high-power multilevel converters. The fact that the behaviour of a pulse-width modulated converter is easy to analyse makes the design of the filter components and calculation of the losses in the converter relatively straightforward. From a control point of view the low-frequency model of a pulse-width modulated converter is simply that of a linear amplifier and basic control loops, usually based on PI or PID controllers, are easy to design.

One application of pulse-width modulation where very high requirements are set on the performance of the control loop is that of pulse-width modulated class-d audio amplifiers. In order to obtain state-of-the art performance loop gains of more than 50 dB are required across the audio band [1]. In this case the simple linear low-frequency model of the pulse-width modulator is not sufficient to obtain the required performance and more advanced models [2], that take the sampling effect of the pulse-width modulator into account, have been investigated. The issue of the influence of ripple feedback on the small-signal gain of the PWM control loop and finding efficient ways to compensate for this also has to be dealt with [3], [4].

Modulation theory has been a major research area in power electronics for over four decades. Sinusoidal pulse-width modulation (SPWM) has been studied since the 1950s. The first analysis of the harmonics generated by naturally sampled pulse-width modulation can be found in [5]. The geometric model that is presented in this textbook is an innovative application of periodic waveforms of two variables and was based on unpublished works of Bennett. This method of deriving a double Fourier series expansion for the PWM signal has since become the basis on which most further research is based. The geometric method of [5] does rely on a certain amount of three-dimensional insight to construct the ‘walls’ and requires a knowledge of double Fourier series expansions. The work of Holmes and Lipo [6] is a valuable resource for almost all of the possible variations on the theme of pulse-width modulation based on this geometric method first introduced by Black. It analyses advanced pulse-width modulation strategies including space-vector modulation [7], [8], [9] as well as applications of pulse-width modulation to multilevel converters [10], [11], [12] where some of the harmonic side-bands are eliminated through phase-shifting of the carriers.

An important question is how to analyse the PWM spectrum in the more general case where the modulating waveform is not a simple sinusoid. In [13] Holmes included a third harmonic in the modulating waveform. This presented an important advance since third-harmonic injection [14] is a simple way of achieving over-modulation in three-phase converters without distorting the output voltage. In work by Deslauriers, Avdiu and Ooi [15] a general analytic method, based on the geometric method of Black, of predicting the spectrum for any modulating waveform with a Fourier series expansion and taking a finite number of harmonics into account was presented for a naturally sampled double-side pulse-width modulator. Furthermore, conditions for signal recovery similar to the Nyquist theorem or Carson’s rule for FM modulation were derived.

The geometric method of [5] provides an analytical way of calculating the harmonics of the PWM waveforms and results in closed form solutions for a number of special cases of the modulating waveform. Unfortunately it provides little insight into the PWM process and the mechanisms that generate the harmonic sidebands. Since it is based on Fourier series methods it is only applicable to the case where the modulating waveform is periodic. In this booklet a new approach to analyse the behaviour of a single-sided pulse-width modulator is presented. By using elementary

methods it is shown how the pulse-width modulated waveforms can be decomposed into the original modulating waveform, a copy of the sawtooth carrier and a sawtooth function. By applying the standard one-dimensional Fourier series representation of the sawtooth function an equivalent model of the pulse-width modulator is derived. The model clearly identifies the non-linearities that generate the harmonic sidebands and shows how these sidebands are modulated onto sinusoidal carriers at integer multiples of the switching frequency to generate the PWM spectrum. The special case of sinusoidal modulation is easily dealt with and the well-known equations for the harmonics are derived in a few simple steps. No knowledge of the geometric method of [5] or of two-dimensional Fourier series expansions is required. The new model predicts the Fourier transform of the PWM signal. It applies to any modulating waveform and no assumption regarding its periodicity has to be made. The only restriction is that the modulating waveforms must be limited to 1 or -1 in the case of over-modulation. It thus extends the existing methods based on those of Bennett and Black, which only applies to periodic modulating waveforms, to include aperiodic modulating waveforms.

A new simulation strategy can easily be derived once the non-linearity that generates the PWM sidebands has been identified. The proposed simulation strategy does not require the exact calculation of the intersection between the modulating waveform and the carrier, nor does it require very fine time quantisation of the PWM signal.

In the second part of the booklet the model is applied to the case where the modulating waveform consists of a finite sum of different modulating waveforms. It is shown that addition of modulating waveforms in the time domain translates into convolution of the PWM sidebands in the frequency domain. The resulting model is intuitively easy to understand and provides an accurate way of predicting the PWM spectrum in the case where the modulating waveform is a band-limited periodic waveform.

In the final part of the booklet regular sampled single-sided PWM is considered. The interaction of the sampling process and the PWM non-linearity is studied and a general expression for the Fourier transform of a regular sampled PWM waveform is derived. When adapting the original method of Bennett and Black to include sampled PWM [6] a special trick is used (y is replaced by $y' + \left(\frac{\omega_0}{\omega_c}\right)x$) in the construction of the unit cell. This trick only works if the modulating waveform is periodic. Using the techniques developed here it is again shown how the assumption that the modulating waveform is periodic can be dropped.

II. A SIMPLE APPROACH TO THE PWM SPECTRUM

Consider the PWM pulse train $p(t)$ in Figure 1(b) generated by comparing the PWM modulating waveform $f(t)$ with the sawtooth carrier $\text{st}(\omega_s t)$ of Figure 1(a), where ω_s is the switching frequency. This pulse train can be decomposed as the sum of three functions

$$p(t) = f(t) - \text{st}(\omega_s t) + \text{st}(\omega_s t - \pi f(t) + \pi), \quad (1)$$

as shown in Figure 1(c). In order to prove this statement it is only necessary to consider $p(t)$ over the interval $-\frac{T_s}{2} \leq t \leq \frac{T_s}{2}$. The remainder of the proof follows from the fact that the sawtooth carrier is periodic.

Note that t_x is the time instant when $f(t)$ intersects $\text{st}(\omega_s t)$. Now consider the decomposition of equation (1):

- During the interval $-\frac{T_s}{2} \leq t \leq t_x$ it is easy to see that $-\pi < \omega_s t - \pi f(t) + \pi < \pi$ which implies

$$f(t) - \text{st}(\omega_s t) + \text{st}(\omega_s t - \pi f(t) + \pi) = f(t) - \frac{1}{\pi} \omega_s t + \frac{1}{\pi} (\omega_s t - \pi f(t) + \pi) = 1.$$

Similarly for $t_x \leq t \leq \frac{T_s}{2}$ it is easy to see that $\pi < \omega_s t - \pi f(t) + \pi < 3\pi$ which implies that

$$f(t) - \text{st}(\omega_s t) + \text{st}(\omega_s t - \pi f(t) + \pi) = f(t) - \frac{1}{\pi} \omega_s t + \frac{1}{\pi} (\omega_s t - \pi f(t) + \pi - 2\pi) = -1.$$

This argument can easily be adapted to the case where the modulating waveform $p(t)$ intersects the carrier not once, but a finite number of times per switching period.

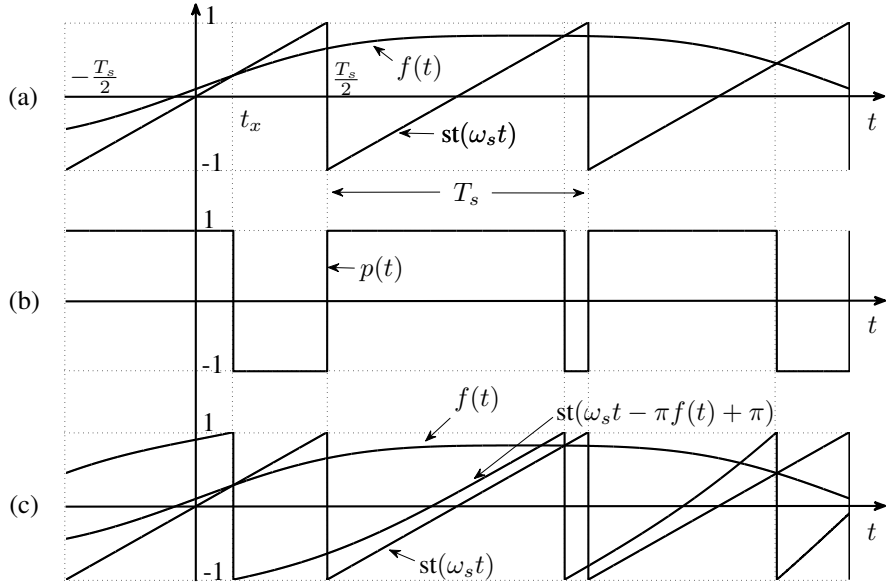


Fig. 1. Expanding the PWM pulse train into sawtooth functions.

The next step is to expand the sawtooth function $st(\theta)$ into its exponential Fourier series representation:

$$st(\theta) = \frac{j}{\pi} \sum_{\substack{m=-\infty \\ m \neq 0}}^{\infty} \frac{e^{jm(\theta+\pi)}}{m} \quad (2)$$

Replacing the second sawtooth functions in equation (1) with its Fourier series expansions results in:

$$p(t) = f(t) - st(\omega_s t) + \frac{j}{\pi} \sum_{\substack{m=-\infty \\ m \neq 0}}^{\infty} \frac{1}{m} e^{jm(\omega_s t - \pi f(t))}. \quad (3)$$

It should be noted that it is possible to derive equation (3) through a modification of the geometric method of [5]. The original method of [5] only applies to periodic modulating waveforms since it is based on a Fourier series representation of the background function along both axes. However, by taking the Fourier transform along the y -axis and the Fourier series representation along the x -axis it can be adopted to accommodate aperiodic modulating waveforms.

Another alternative approach to calculate the spectrum of sinusoidal naturally sampled PWM is the method of duty cycle variation [16], [17] and [18]. In this method it is assumed that the reference signal remains constant over a switching period. The method of duty cycle variation produces the correct result, at least in the case of sinusoidal modulation. However, this is rather coincidental since the premise on which it is based is an approximation which is only possible to fully justify if the modulating waveform changes infinitely slowly compared to the frequency of the carrier. The method proposed in this booklet does not rely on any approximations.

Rewriting equation (3) in trigonometric form yields:

$$p(t) = f(t) - st(\omega_s t) + \frac{2}{\pi} \sum_{m=1}^{\infty} \frac{1}{m} \sin m(\omega_s t - \pi f(t)) \quad (4)$$

$$= f(t) - st(\omega_s t) + \frac{2}{\pi} \sum_{m=1}^{\infty} \frac{1}{m} (\cos(\pi m f(t)) \sin m(\omega_s t) - \sin(\pi m f(t)) \cos m(\omega_s t)) \quad (5)$$

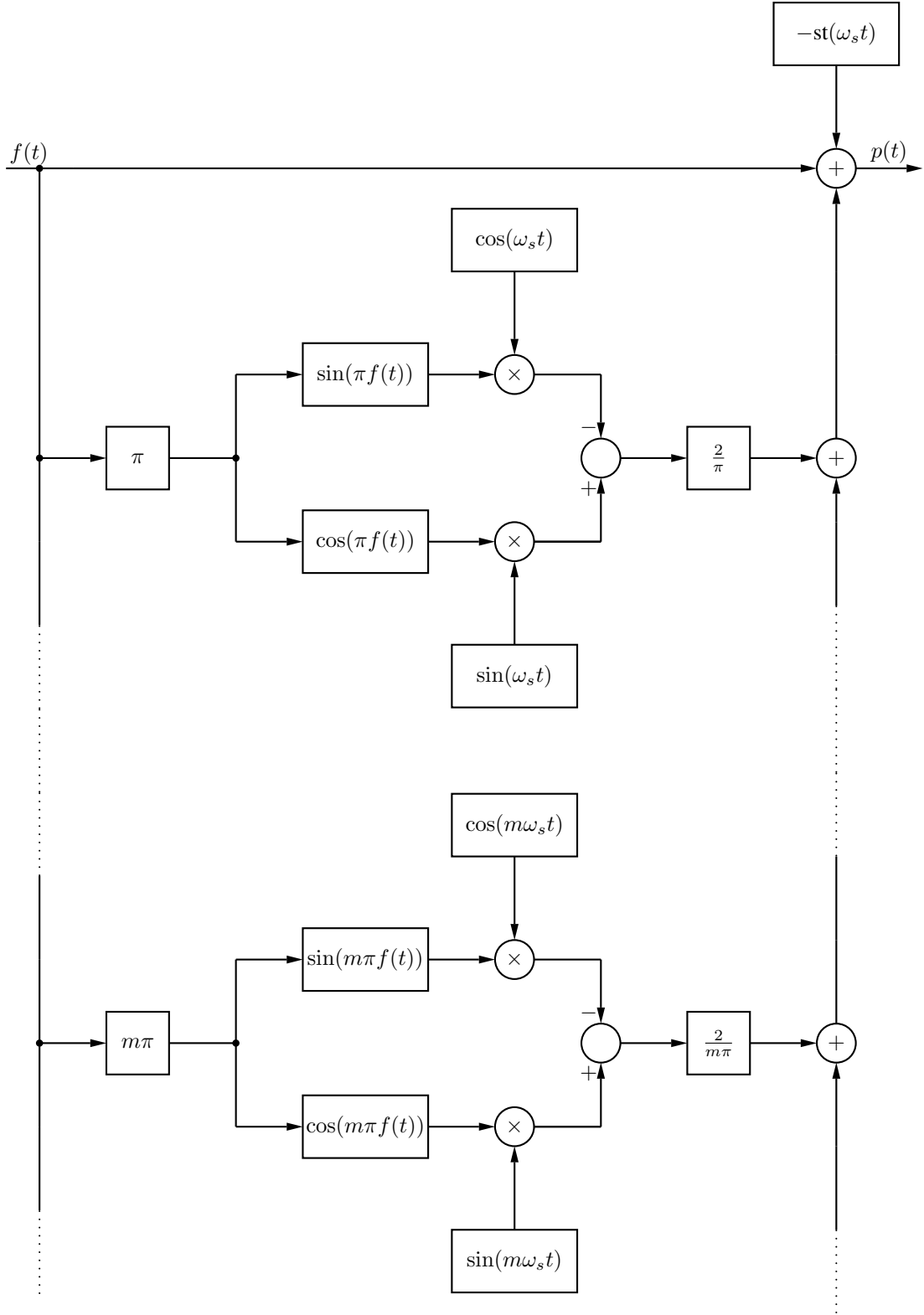


Fig. 2. Equivalent block diagram of the single-sided pulse-width modulator in trigonometric form.

Figure 2 shows the equivalent block diagram of the single-sided pulse-width modulator based on this series expansion of $p(t)$. It shows that the pulse-width modulator is equivalent to a sequence of phase modulators, with each phase modulator producing a sideband of harmonics around an integer multiple m of the switching frequency.

By studying this block diagram it is evident that $p(t)$ consists of the following:

- A copy of the original modulating waveform $f(t)$.
- An inverted copy $-st(\omega_s t)$ of the sawtooth carrier.
- The output of the first phase modulator which operates in the following way: The modulating waveform $f(t)$ is multiplied by π and passed through the cosine non-linearity. The result is modulated onto the carrier $\sin(\omega_s t)$. In a similar way modulating waveform $f(t)$ is multiplied by π and passed through the sine non-linearity. The result is modulated onto the carrier $\cos(\omega_s t)$. The second signal is subtracted from the first and the result is multiplied by the constant $\frac{2}{\pi}$.
- The other phase modulators operate in the same way, except that the modulating waveform is multiplied by $m\pi$ before passing it through the sine and cosine non-linearities and are modulated onto carriers with frequency $m\omega_s t$. The results are subtracted and multiplied by $\frac{2}{m\pi}$.

In order to derive an expression for the Fourier transform of $p(t)$, let $F_{em}(\omega)$ represent the Fourier transform of $e^{-jm\pi f(t)}$, i.e.

$$F_{em}(\omega) = \mathcal{F}\left\{e^{-jm\pi f(t)}\right\}. \quad (6)$$

By taking the Fourier transform of (3) and using the fact that multiplication by $e^{jm\omega_s t}$ corresponds to a frequency shift by $m\omega_s$ in the frequency domain, the Fourier transform $P(\omega)$ of the PWM pulse train $p(t)$ can be written as:

$$P(\omega) = F(\omega) - ST(\omega) + \frac{j}{\pi} \sum_{\substack{m=-\infty \\ m \neq 0}}^{\infty} \frac{1}{m} F_{em}(\omega - m\omega_s) \quad (7)$$

Figure 3 shows the equivalent block diagram in exponential form corresponding to equation (3). In this representation it can be seen that the sidebands are produced by the $e^{-jm\pi f(t)}$ non-linearity. Modulating the output of this non-linearity onto the carrier $e^{jm\omega_s t}$ is equivalent to shifting the spectrum $F_{em}(\omega)$ by $m\omega_s$ along the frequency axis.

Unlike the double Fourier series methods, equation (7) correctly describes $P(\omega)$, even if the modulating waveform $f(t)$ is not periodic. To illustrate this consider the aperiodic modulating waveform

$$f(t) = \left(\frac{\sin(\omega_0 t)}{\omega_0 t} \right)^2$$

with Fourier transform

$$F(\omega) = \frac{\pi}{\omega_0} \text{tri}\left(\frac{\omega}{2\omega_0}\right),$$

where $\text{tri}(x)$ is the triangular pulse defined by

$$\text{tri}(x) = \begin{cases} 1 - |x| & \text{if } |x| < 1 \\ 0 & \text{otherwise.} \end{cases}$$

Figure 4 shows the PWM spectrum for $\omega_0=2000$ rad/s and a switching frequency of 10 kHz up the third sideband. In order to focus on the relatively small sidebands the y-axis is scaled in such a way that the large harmonics at multiples of the switching frequency fall outside the figure.

The four smaller graphs show the magnitudes of the Fourier transforms $|F_{em}|$ of the output signals of the $e^{-j\pi mf(t)}$ non-linearities. In order to calculate these the Fourier transforms of $e^{-jm\pi f(t)}$ were calculated for $m = 1, 2, 3$ by making use of the Fast Fourier Transform algorithm. These are shifted in frequency and multiplied by $\frac{j}{m\pi}$ to produce the sidebands of $P(\omega)$, as described by equation (7). This provides a very quick and efficient method for calculating the PWM spectrum.

The sideband around 0 Hz in Figure 4 is simply the Fourier transform of $f(t)$. The sidebands around multiples of the switching frequency are essentially distorted copies of this triangular Fourier transform. As m increases the sidebands get wider as a result of the factor m in the $e^{-jm\pi f(t)}$ non-linearity, but decrease in magnitude due to the

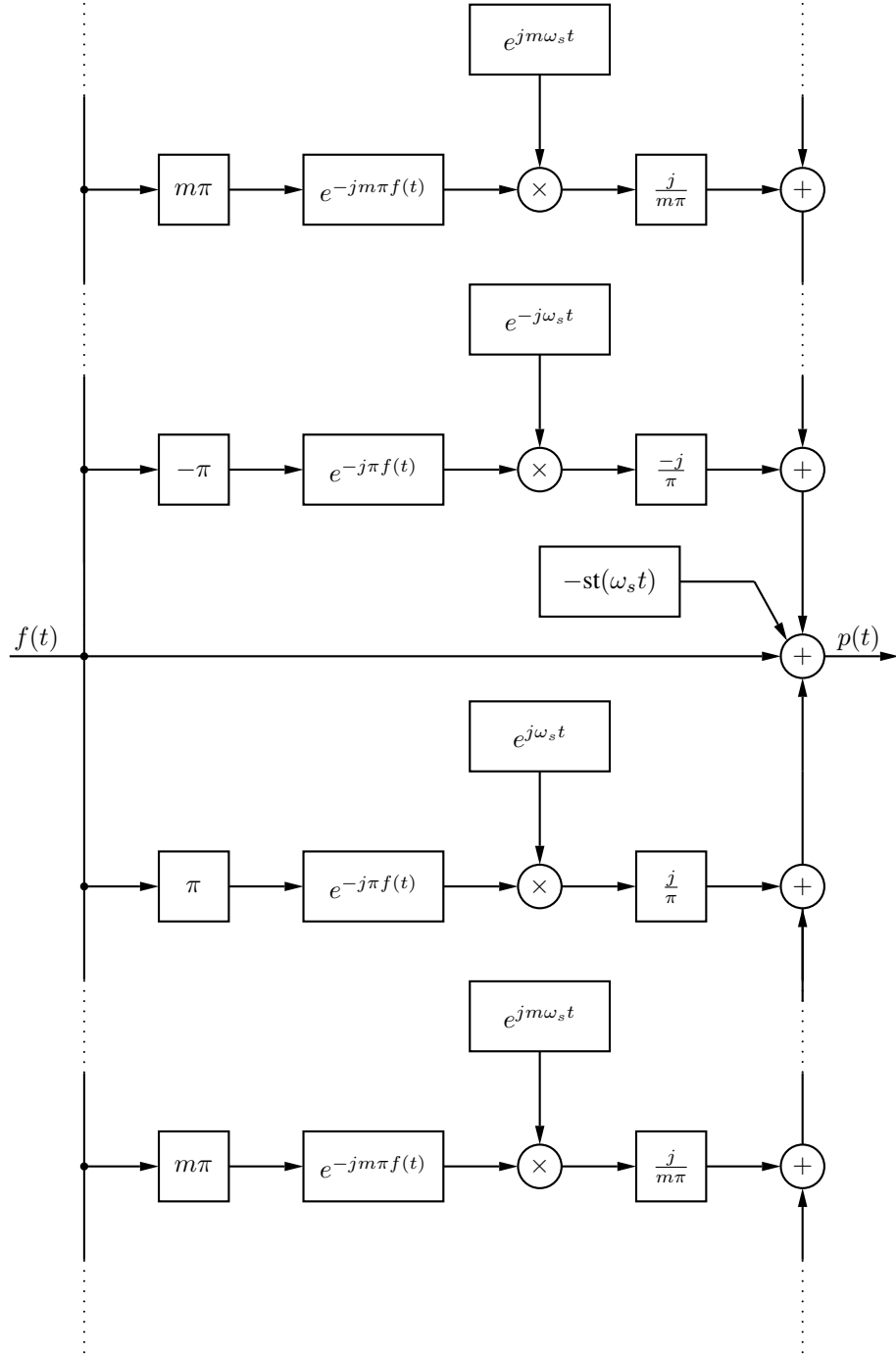


Fig. 3. Equivalent block diagram of the single-sided pulse-width modulator in complex exponential form.

multiplication by $\frac{j}{m\pi}$. The harmonics at integer multiples of the switching frequency consist of the harmonics of the sawtooth carrier as well as the DC components of $e^{-jm\pi f(t)}$.

The bottom graph of Figure 4 also shows the result of a time-domain simulation of the PWM spectrum, indicated by dotted lines. The exact intersections between $f(t)$ and the sawtooth carrier were calculated by using the Newton-Raphson method. The two sets of results are virtually indistinguishable with the time-domain simulation showing near-perfect agreement with the theoretically predicted spectrum.

Over the past number of years a number of methods for the efficient simulation of the spectra of PWM signals

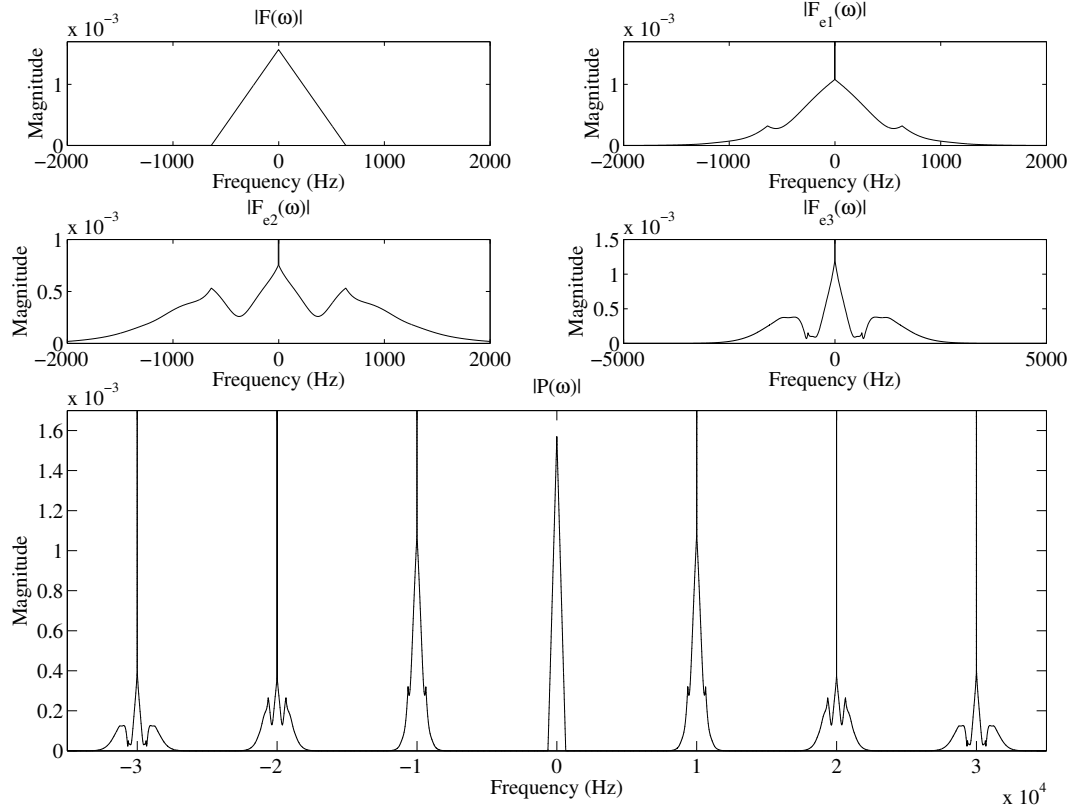


Fig. 4. PWM spectrum with an aperiodic modulating waveform.

have been studied [19], [17] and [6] (Appendix 5). Equation (7) provides an easy and efficient way to calculate the PWM spectrum of an arbitrary signal over a number of sidebands. Standard numerical methods, like the Fast Fourier Transform, can be used to calculate the spectrum of $F_{e_m}(\omega)$ for as many values of m as required. The results simply have to be shifted in frequency and added to obtain the PWM spectrum. The proposed method does not require the exact calculation of the intersection between the modulating waveform and the carrier, nor does it require very fine time quantisation of the PWM signal.

III. SINUSOIDAL MODULATION

Next the special case where $f(t)$ is sinusoidal of the form $f(t) = m_a \cos(\omega_0 t)$, where $0 \leq m_a \leq 1$ is the modulation index, is considered.

Applying the Jacobi-Anger identity [20]

$$e^{-jm\pi m_a \cos(\omega_0 t)} = \sum_{n=-\infty}^{\infty} (j)^n J_n(-m\pi m_a) e^{jn\omega_0 t}, \quad (8)$$

to equation (3) results in the well-known double Fourier series expansion

$$p(t) = f(t) - st(\omega_s t) - \sum_{m=1}^{\infty} \sum_{n=-\infty}^{\infty} \frac{2}{m\pi} J_n(m\pi m_a) \sin \left((n\omega_0 + m\omega_s)t - \frac{n\pi}{2} \right), \quad (9)$$

where $J_n(x)$ is the n 'th order Bessel function of the first kind. This is identical to the double Fourier series expansion derived through the method of [5].

IV. SUM OF MODULATING WAVEFORMS

As mentioned in the introduction, the important question of studying the spectrum of the PWM signal in the case where the modulating waveform consists of a finite sum of signals has only been partially solved for triangular PWM [15], [21], resulting in complicated solutions. In this section it is shown that addition in the time-domain results in convolution of the sidebands in the frequency domain.

Consider the case where the modulating waveform is a finite sum of signals

$$f(t) = \sum_{k=1}^K f_k(t).$$

According to equation (6)

$$\begin{aligned} F_{e_m}(\omega) &= \mathcal{F} \left\{ \exp \left(-jm\pi \sum_{k=1}^K f_k(t) \right) \right\} \\ &= \mathcal{F} \left\{ \prod_{k=1}^K e^{-jm\pi f_k(t)} \right\}. \end{aligned}$$

Since multiplication in the time domain corresponds to convolution in the frequency domain

$$\begin{aligned} F_{e_m}(\omega) &= \mathcal{F} \left\{ e^{-jm\pi f_1(t)} \right\} * \mathcal{F} \left\{ e^{-jm\pi f_2(t)} \right\} * \dots * \mathcal{F} \left\{ e^{-jm\pi f_K(t)} \right\} \\ &= F_{1e_m}(\omega) * F_{2e_m}(\omega) * \dots * F_{Ke_m}(\omega), \end{aligned}$$

where

$$F_{ke_m}(\omega) = \mathcal{F} \left\{ e^{-jm\pi f_k(t)} \right\} \quad \text{for } k = 1, \dots, K.$$

According to equation (7) the Fourier transform of the resulting PWM pulse train is given by

$$P(\omega) = F(\omega) - ST(\omega) + \frac{j}{\pi} \sum_{\substack{m=-\infty \\ m \neq 0}}^{\infty} \frac{1}{m} \{ F_{1e_m}(\omega - m\omega_s) * F_{2e_m}(\omega - m\omega_s) * \dots * F_{Ke_m}(\omega - m\omega_s) \}. \quad (10)$$

This means that a summation of modulating waveforms in the time domain translates into a frequency-domain convolution of the respective sidebands.

In order to illustrate this Figure 5 shows the PWM spectra with an modulating waveform $f(t)$ consisting of sinusoidal signals at 50 Hz and 150 Hz, i.e.

$$f(t) = f_1(t) + f_2(t),$$

with

$$f_1(t) = 0.5 \sin(2\pi \cdot 50t) \quad \text{and} \quad f_2(t) = 0.3 \sin(2\pi \cdot 150t).$$

The switching frequency is 2 500 Hz.

The first row of graphs shows the Fourier transforms $F_1(\omega)$, $F_2(\omega)$ and $F_1(\omega) + F_2(\omega)$. The first two graphs of every row were generated by calculating the FFT of the respective time-domain functions. The third graph was generated by using Matlab's convolution function. The second row shows the Fourier transforms of output of the first exponential non-linearity $F_{1e_1}(\omega)$ and $F_{2e_1}(\omega)$ as well as the frequency domain convolution of the two. This convolution is multiplied by $\frac{j}{\pi}$, shifted in frequency by $\pm\omega_s$ to form the first sideband of the PWM spectrum of $f(t)$. Similarly, the third and fourth rows of graphs show the outputs of the second and third exponential nonlinearities which are multiplied by $\frac{j}{m\pi}$, shifted in frequency by $\pm m\omega_s$ to form the second and third sidebands.

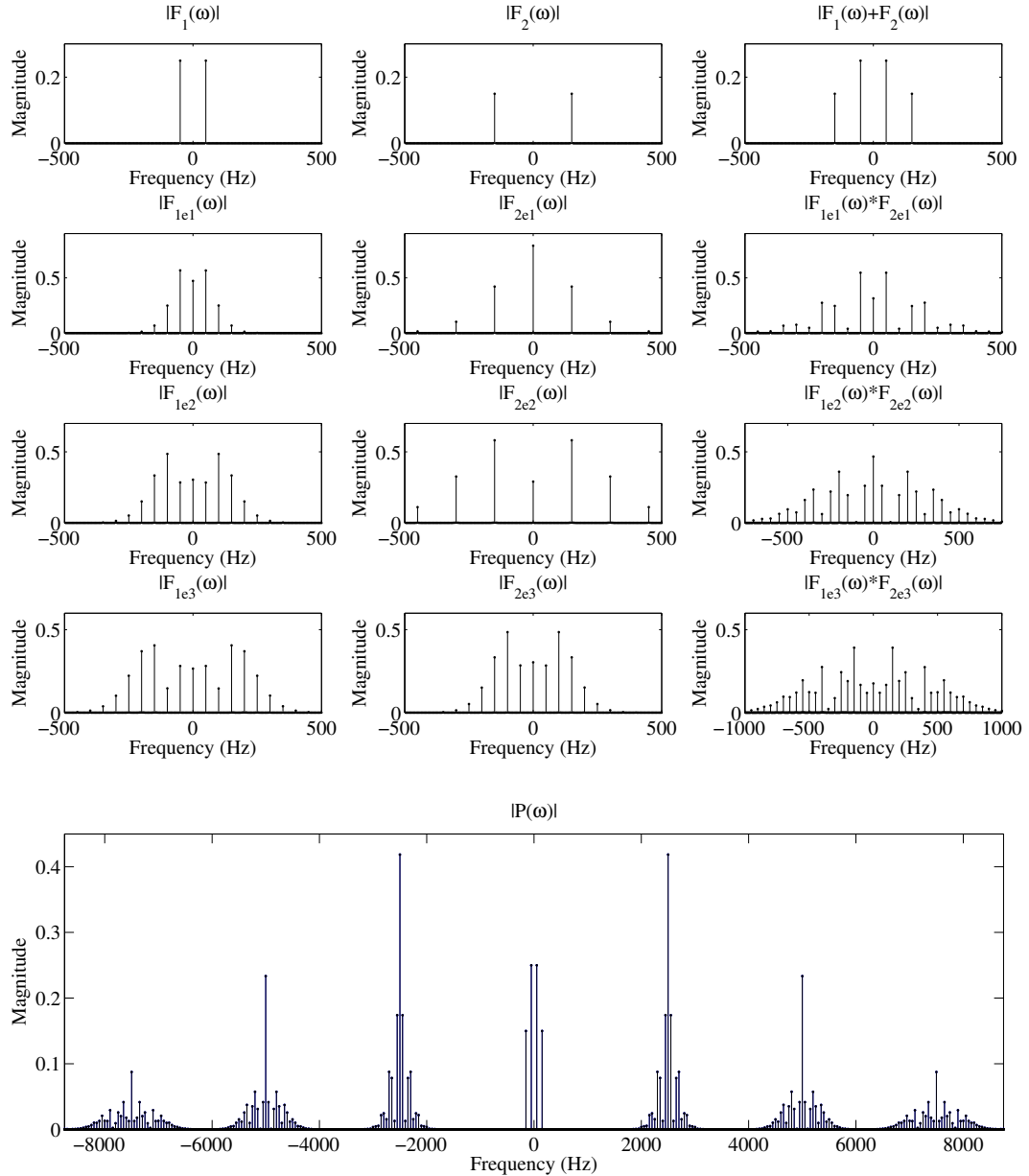


Fig. 5. PWM spectrum with a two-tone modulating waveform.

A time-domain simulation of the actual PWM signal was again performed to verify the validity of the theory. The results are plotted on the bottom graph of Figure 5. It shows almost exact agreement with the theoretical results and are impossible to distinguish on the graph.

In [15] a condition similar to Carson's rule for frequency modulation [22] was derived for double-sided PWM. This condition applies to the case where the modulating signal $f(t)$ consists of one main sinusoid $g_1(t)$ at frequency ω_m and a number of smaller sinusoids at frequencies $\omega_1, \dots, \omega_{upper}$ superimposed on it. The condition states that the modulating signal can be recovered from the PWM pulse train through low-pass filtering provided that

$$2\omega_{upper} + \omega_m < \omega_s.$$

A similar rule can be derived from equation (10) for single-sided modulation in the case where a small arbitrary band-limited signal $f_2(t)$ with bandwidth ω_2 is superimposed on a sinusoid $f_1(t)$ with frequency ω_1 , where $\omega_2 > \omega_1$.

First consider the first sideband of harmonics ($m=1$) of F_{1e_1} as characterised by equation (9).

By studying the properties of the Bessel functions of the first kind it can be observed that $|J_n(x)| < 0.1$ for x in the interval $[-\pi, \pi]$ and for $n \geq 5$. Hence only the first four sideband harmonics of F_{1e_1} are considered to be significant. (Note that the sidebands decay faster for two-sided PWM and that all the odd order harmonics are zero for the first sideband.)

Next consider the first sideband F_{2e_1} of $f_2(t)$. Truncating the Taylor series of $e^{-j\pi f_2(t)}$ results in the following small-signal approximation:

$$e^{-j\pi f_2(t)} \approx 1 - j\pi f_2(t)$$

Hence the only effect of the exponential non-linearity associated with the first sideband on the magnitude of the Fourier transform is to add an impulse at zero rad/s in the frequency domain.

By combining these two observations the lowest significant harmonic of the first sideband will occur at a minimum frequency of $\omega_s - (4\omega_1 + \omega_2)$. An approximate condition for signal recovery through low-pass filtering for single-sided PWM is thus given by:

$$\omega_2 < \frac{1}{2}\omega_s - 2\omega_1$$

V. SAWTOOTH CARRIER REGULAR SAMPLED PWM

Sampled pulse-width modulation is used in most digital implementations of PWM. The conventional method samples the modulating waveform once per switching period, at the falling edge of the sawtooth carrier. However, much higher sampling ratios are possible and minimises the delay associated with digital PWM. When using higher sampling ratios careful attention has to be paid to the effect of ripple-feedback [1]. While the analysis presented here can easily be adapted to higher sampling ratios only the conventional method will be discussed here.

For a sawtooth carrier the sampling occurs at the falling edge of the sawtooth carrier and the value of the modulating waveform is held constant for the rest of the switching period. This is equivalent to inserting a sample-and-hold register between the modulating waveform $f(t)$ and the pulse-width modulator, or equivalently placing a sample-and-hold register at the input of each of the branches in Figure 3. Figure 6(a) shows the m 'th branch of Figure 3 with the sample-and-hold (S/H) register included at the input of the branch. Due to the nature of the $e^{-jm\pi f(t)}$ non-linearity, in particular the fact that it has no memory, the sample-and-hold register and the non-linearity can be interchanged as shown in Figure 6(b).

It is well known [23] that the sample-and-hold register is equivalent to multiplication by an impulse train $it(t)$ (with the impulses located at the sampling instances) followed by a zero-order filter as shown in Figure 6(c). The Fourier series expansion of the impulse train is given by:

$$it(t) = \frac{1}{T_s} \sum_{k=-\infty}^{\infty} e^{-jk\pi} e^{jk\omega_s t}$$

and the transfer function ZOH(ω) of the zero-order-hold filter is given by:

$$\text{ZOH}(\omega) = \frac{1}{j\omega} (1 - e^{-j\omega T_s}) = T_s e^{-j\omega T_s/2} \frac{\sin \frac{\omega T_s}{2}}{\frac{\omega T_s}{2}}$$

Since multiplication by $e^{jk\omega_s t}$ in the time domain corresponds to a frequency shift by $k\omega_s$ in the frequency domain, the Fourier transform $V_m(\omega)$ of $v_m(t)$ is given by

$$V_m(\omega) = \frac{1}{T_s} \sum_{k=-\infty}^{\infty} e^{-jk\pi} F_{em}(\omega - k\omega_s).$$

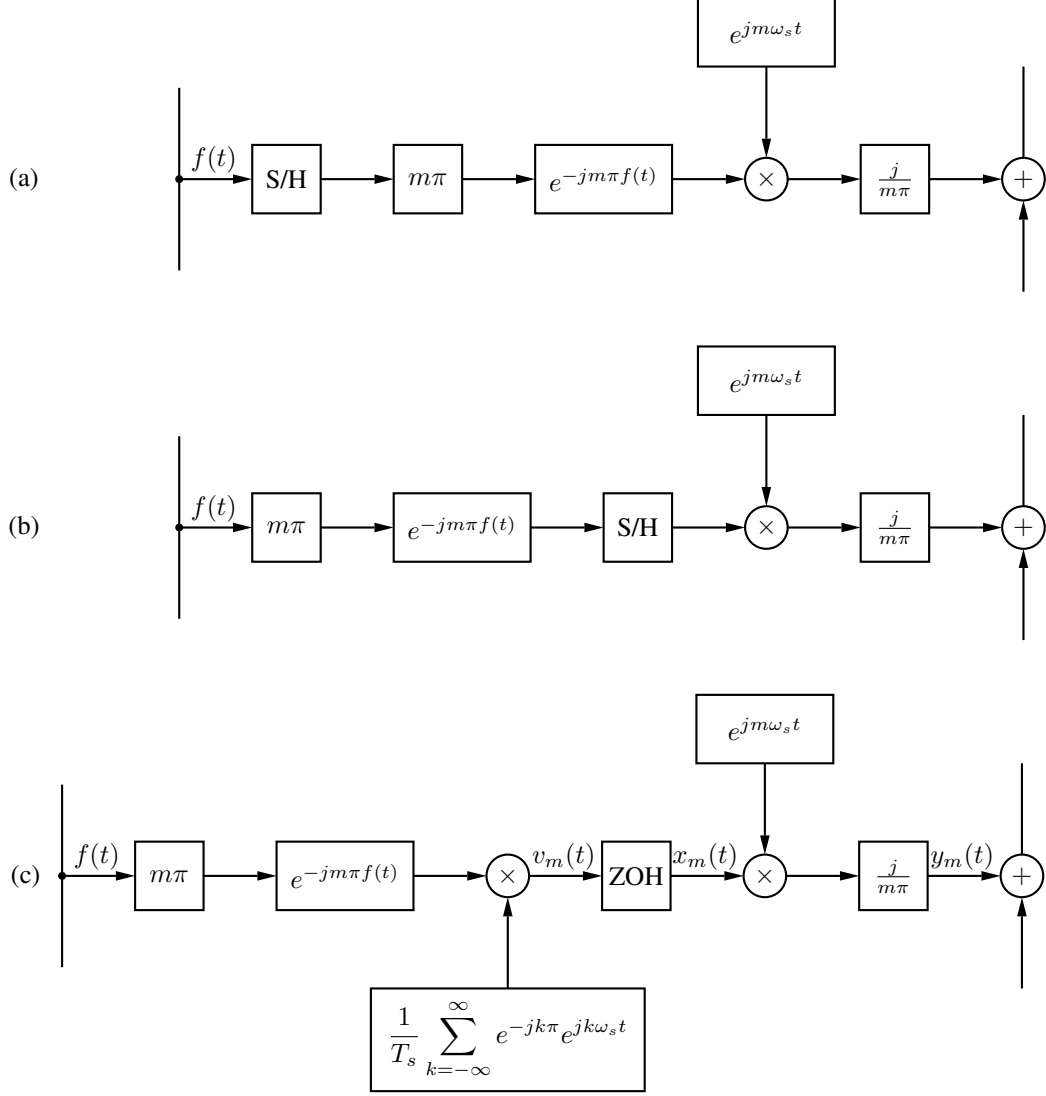


Fig. 6. Three equivalent versions of sampled PWM. (a) Sample-and-hold at the input of every branch; (b) Sample-and-hold interchanged with PWM non-linearity; (c) Sampling represented by multiplication by an impulse train and zero-order-hold filter.

By applying the transfer function of the zero-order-hold filter, the Fourier transform of $x_m(t)$ is given by

$$X_m(\omega) = \frac{1}{T_s} \left[\frac{1 - e^{-j\omega T_s}}{j\omega} \right] \sum_{k=-\infty}^{\infty} e^{-jk\pi} F_{em}(\omega - k\omega_s).$$

Finally, by again making use of the fact that multiplication by $e^{jm\omega_s t}$ in the time domain corresponds to a frequency shift by $m\omega_s$ in the frequency domain, the Fourier transformer of $y_m(t)$ is given by

$$Y_m(\omega) = \frac{j}{m\pi T_s} \left[\frac{1 - e^{-j(\omega - m\omega_s)T_s}}{j(\omega - m\omega_s)} \right] \sum_{k=-\infty}^{\infty} e^{-jk\pi} F_{em}(\omega - (k + m)\omega_s). \quad (11)$$

In order to illustrate the principles involved, Figure 7 shows the frequency-domain sidebands for the case $m=2$. In this case $f(t) = 0.8 \cos(\omega_0 t)$ with $\omega_0 = 50$ Hz and a switching frequency of 2.5 kHz. The top graph shows the Fourier transform of the output of the PWM non-linearity. The sampler multiplies this signal by $\frac{1}{T_s}$ and generates images at integer multiples of the switching frequency. The zero-order-hold filter is a low-pass sinc filter with zeros located at integer multiples of the switching frequency. Finally the multiplication by $e^{jm\omega_s t}$ shifts the spectrum to

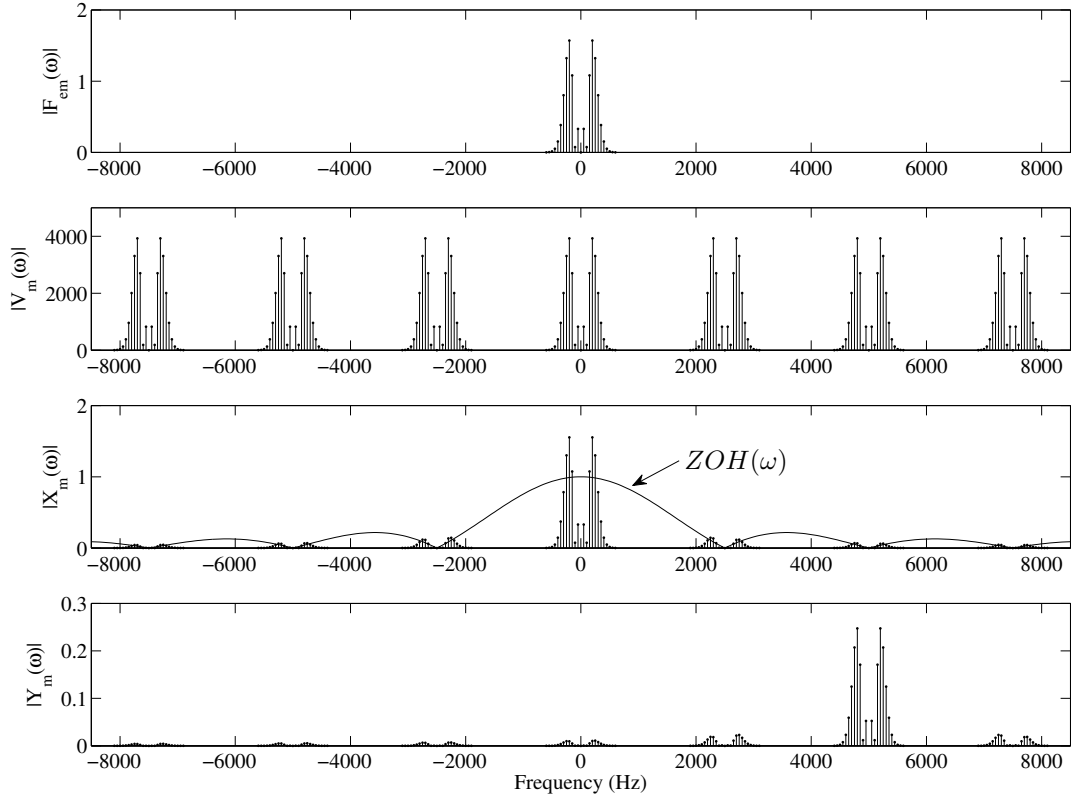


Fig. 7. Spectra of the signals in the second branch of the regularly sampled pulse-width modulator.

the right by $m\omega_s$. The PWM output signal consists of the sum of the output signals of all the different branches ($m = \pm 1, \pm 2, \dots$) as well as a sampled-and-held copy of the original modulating waveform $f(t)$ which corresponds to the case $m = 0$. This model of the regular sampled pulse-width modulator clearly shows how baseband harmonics are generated.

By adding and regrouping the terms of equation (11) an expression for the Fourier transform of the modulator output signal $p(t)$ that separates the Fourier transform into distinct sidebands can be derived:

$$P(\omega) = ST(\omega) + \begin{cases} F(0) & \text{if } \omega = 0 \\ \frac{j}{m\pi} F_{em}(0) & \text{if } \omega = m\omega_s, \text{ where } m \text{ is a non-zero integer} \\ j \frac{e^{-j\pi\frac{\omega}{\omega_s}}}{\pi\frac{\omega}{\omega_s}} \sum_{q=-\infty}^{\infty} e^{-jq\pi} \int_{-\infty}^{\infty} e^{-j\pi\frac{\omega}{\omega_s} f(t)} e^{-j(\omega-q\omega_s)t} dt & \text{if } \omega \neq 0 \text{ and is not an integer multiple of } \omega_s \end{cases} \quad (12)$$

The details of the derivation of this equation are contained in Appendix A. Equation (12) is a general equation whereby the Fourier transform of the regular sampled PWM output signal can be calculated (at least numerically) for any modulating waveform $f(t)$. It is interesting to note that only the DC-component of the original modulating waveform is left undistorted.

When using the geometric method of [5] a simple and elegant modification to the geometric method for natural sampled PWM is used to analyse sampled PWM in the case where the modulating waveform is periodic ([6] section 3.6.1). It is, however, unclear how to adapt this modification in the case where the modulating waveforms is not periodic. In contrast the equation above applies to aperiodic signals as well as periodic signals.

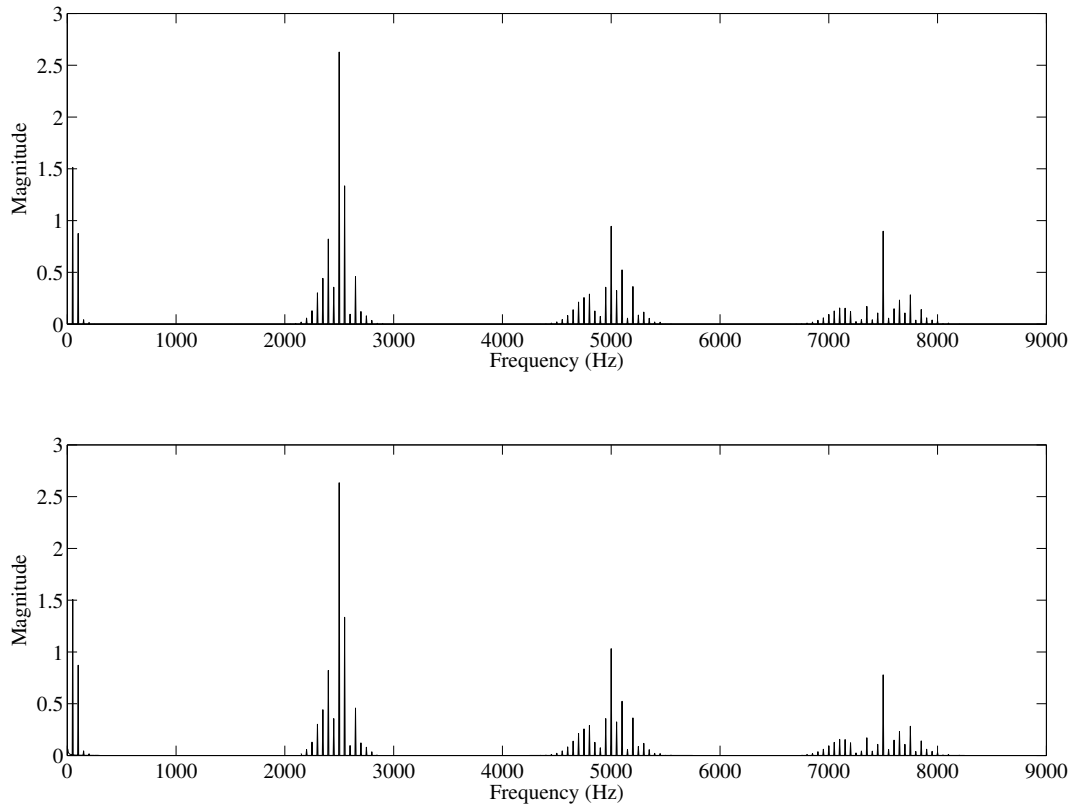


Fig. 8. Spectra of a finite-duration two-tone regularly sampled PWM signal. Top: Result of time-domain simulation. Bottom: Direct integration of equation (12).

In order to verify the validity of equation (12) a time domain simulation of the PWM spectrum of the following finite-duration modulating waveform was performed:

$$f(t) = \begin{cases} 0 & \text{if } t < -3.0002 \text{ s} \\ 0.5 \sin(100\pi t) + 0.3 \sin(200\pi t) & \text{if } -3.0002 \leq t \leq 3.0002 \text{ s} \\ 0 & \text{if } t > 3.0002 \text{ s} \end{cases}$$

The switching frequency f_s for this simulation is 2 500 Hz. The top graph of Figure 8 shows the results of a time-domain simulation where the PWM spectrum was obtained by numerically adding the results of the Fourier transforms of each of the individual PWM pulses. The bottom graph was obtained by direct numerical integration of equation (12). The two spectra show near-perfect agreement, and small differences between the two can be attributed to numerical inaccuracies.

Next consider the case of sinusoidal modulation with $f(t) = m_a \cos(\omega_o t)$ and $m_a \leq 1$. By using the Jacobi-Anger identity (8) and regrouping terms it is possible to show that

$$\begin{aligned} p(t) = & \frac{2}{\pi} \sum_{m=1}^{\infty} \frac{1}{m} (\cos(m\pi) - J_0(m\pi m_a)) \sin(m\omega_s t) \\ & + \frac{2}{\pi} \sum_{q=1}^{\infty} \sum_{n=-\infty}^{\infty} \frac{J_n(\pi m_a(n\frac{\omega_0}{\omega_s} + q))}{n\frac{\omega_0}{\omega_s} + q} \cos \left((n\omega_0 + q\omega_s)t + \frac{\pi}{2} - n\pi \left(\frac{1}{2} + \frac{\omega_0}{\omega_s} \right) \right) \end{aligned}$$

$$+ \frac{2}{\pi} \sum_{n=1}^{\infty} \frac{J_n(\pi m_a n \frac{\omega_0}{\omega_s})}{n \frac{\omega_0}{\omega_s}} \cos \left(n\omega_0 t + \frac{\pi}{2} - n\pi \left(\frac{1}{2} + \frac{\omega_o}{\omega_s} \right) \right)$$

which corresponds to equation 3.70 of [6].

APPENDIX A : PROOF OF EQUATION (12)

First consider the case where the frequency of interest ω is a non-zero integer multiple $m\omega_s$ of the switching frequency ω_s . Since the zero-order-hold filter has zeros at every non-zero integer multiple of the switching frequency, the only contribution to the modulator output $P(m\omega)$ at this frequency is that of the m 'th branch of Figure 6, with

$$Y_m(m\omega_s) = \frac{j}{m\pi} F_{em}(0) = \frac{j}{m\pi} \int_{-\infty}^{\infty} e^{-jm\pi f(t)} dt. \quad (13)$$

Next consider the case where ω is not an integer multiple of ω_s . Taking the sum over all non-zero values of m results in:

$$\begin{aligned} I(\omega) &= \sum_{\substack{m=-\infty \\ m \neq 0}}^{\infty} \frac{j}{m\pi T_s} \left[\frac{1 - e^{-j(\omega - m\omega_s)T_s}}{j(\omega - m\omega_s)} \right] \sum_{k=-\infty}^{\infty} e^{-jk\pi} F_{em}(\omega - (k+m)\omega_s) \\ &= \frac{1 - e^{-j\omega T_s}}{\pi T_s} \sum_{\substack{m=-\infty \\ m \neq 0}}^{\infty} \sum_{k=-\infty}^{\infty} \frac{e^{-jk\pi} F_{em}(\omega - (k+m)\omega_s)}{m(\omega - m\omega_s)} \end{aligned}$$

Now let $q = k + m$, then

$$\begin{aligned} I(\omega) &= \frac{1 - e^{-j\omega T_s}}{\pi T_s} \sum_{\substack{m=-\infty \\ m \neq 0}}^{\infty} \sum_{q=-\infty}^{\infty} \frac{e^{-j(q-m)\pi} F_{em}(\omega - q\omega_s)}{m(\omega - m\omega_s)} \\ &= \frac{1 - e^{-j\omega T_s}}{\pi T_s} \sum_{q=-\infty}^{\infty} e^{-jq\pi} \sum_{\substack{m=-\infty \\ m \neq 0}}^{\infty} \frac{e^{jm\pi} F_{em}(\omega - q\omega_s)}{m(\omega - m\omega_s)} \\ &= \frac{1 - e^{-j\omega T_s}}{\pi T_s} \sum_{q=-\infty}^{\infty} e^{-jq\pi} \sum_{\substack{m=-\infty \\ m \neq 0}}^{\infty} \frac{e^{jm\pi}}{m(\omega - m\omega_s)} \int_{-\infty}^{\infty} e^{-jm\pi f(t)} e^{-j(\omega - q\omega_s)t} dt \\ &= \frac{1 - e^{-j\omega T_s}}{\pi T_s} \sum_{q=-\infty}^{\infty} e^{-jq\pi} \int_{-\infty}^{\infty} e^{-j(\omega - q\omega_s)t} \sum_{\substack{m=-\infty \\ m \neq 0}}^{\infty} \frac{e^{jm\pi}}{m(\omega - m\omega_s)} e^{-jm\pi f(t)} dt \end{aligned} \quad (14)$$

Now consider the series

$$\begin{aligned} R(\omega) &:= \sum_{\substack{m=-\infty \\ m \neq 0}}^{\infty} \frac{e^{jm\pi}}{m(\omega - m\omega_s)} e^{-jm\pi f(t)} \\ &= \sum_{\substack{m=-\infty \\ m \neq 0}}^{\infty} \frac{1}{\omega} \left(\frac{e^{jm\pi}}{m(1 - \alpha m)} \right) e^{-jm\pi f(t)}, \end{aligned}$$

where $\alpha = \frac{\omega_s}{\omega}$. Expanding the term $\frac{1}{m(1 - \alpha m)}$ into partial fractions, i.e. $\frac{1}{m(1 - \alpha m)} = \frac{1}{m} + \frac{\alpha}{1 - \alpha m}$ results in

$$R(\omega) = \frac{1}{\omega} \sum_{\substack{m=-\infty \\ m \neq 0}}^{\infty} \frac{e^{jm\pi}}{m} e^{-jm\pi f(t)} + \frac{\alpha}{\omega} \sum_{\substack{m=-\infty \\ m \neq 0}}^{\infty} \frac{e^{jm\pi}}{1 - \alpha m} e^{-jm\pi f(t)}.$$

By setting $x = -\pi f(t)$ and taking note of the fact that $-\pi \leq x \leq \pi$ it is clear that R is the sum of two Fourier series:

$$R(\omega) = \frac{1}{\omega} \sum_{\substack{m=-\infty \\ m \neq 0}}^{\infty} \frac{e^{jm\pi}}{m} e^{jm x} + \frac{\alpha}{\omega} \sum_{\substack{m=-\infty \\ m \neq 0}}^{\infty} \frac{e^{jm\pi}}{1 - \alpha m} e^{jm x}. \quad (15)$$

The first series corresponds to the Fourier series expansion of $\text{st}(x)$ given in equation (2). Hence the first term is equal to

$$R_1(\omega) := \frac{\pi}{j\omega} \text{st}(x) = -\frac{\pi f(t)}{j\omega}.$$

The second series

$$\sum_{\substack{m=-\infty \\ m \neq 0}}^{\infty} \frac{e^{jm\pi}}{1-\alpha m} e^{jmx}$$

is the Fourier series expansion of the periodic function

$$h(x) = \frac{\frac{\pi}{\alpha}}{\sin \frac{\pi}{\alpha}} e^{j\frac{x}{\alpha}} - 1$$

with fundamental period $[-\pi, \pi]$. This can be confirmed by calculating the Fourier coefficients of $h(x)$. Hence the second term of equation (15) is given by:

$$R_2(\omega) := \frac{\pi}{\omega} \frac{1}{\sin \left(\frac{\pi \omega}{\omega_s} \right)} e^{-j\frac{\pi f(t)\omega}{\omega_s}} - \frac{\omega_s}{\omega^2}$$

Finally, substituting these expressions for R_1 and R_2 back into equation (14) gives the following expression for $I(\omega)$

$$\begin{aligned} I(\omega) &= \frac{1 - e^{-j\omega T_s}}{\pi T_s} \sum_{q=-\infty}^{\infty} e^{-jq\pi} \int_{-\infty}^{\infty} e^{-j(\omega-q\omega_s)t} R(\omega) dt \\ &= \frac{1 - e^{-j\omega T_s}}{\pi T_s} \sum_{q=-\infty}^{\infty} e^{-jq\pi} \int_{-\infty}^{\infty} e^{-j(\omega-q\omega_s)t} \left(-\frac{\pi f(t)}{j\omega} + \frac{\pi}{\omega} \frac{1}{\sin \left(\frac{\pi \omega}{\omega_s} \right)} e^{-j\frac{\pi f(t)\omega}{\omega_s}} - \frac{\omega_s}{\omega^2} \right) dt \\ &= -\frac{1 - e^{-j\omega T_s}}{j\omega T_s} \sum_{q=-\infty}^{\infty} e^{-jq\pi} \int_{-\infty}^{\infty} f(t) e^{-j(\omega-q\omega_s)t} dt + j \frac{e^{-j\pi \frac{\omega}{\omega_s}}}{\pi \frac{\omega}{\omega_s}} \sum_{q=-\infty}^{\infty} e^{-jq\pi} \int_{-\infty}^{\infty} e^{-j\pi \frac{\omega}{\omega_s} f(t)} e^{-j(\omega-q\omega_s)t} dt \\ &\quad - \frac{1 - e^{-j\omega T_s}}{j\omega T_s} \sum_{q=-\infty}^{\infty} e^{-jq\pi} \int_{-\infty}^{\infty} \frac{\omega_s}{\omega^2} e^{-j(\omega-q\omega_s)t} dt \end{aligned}$$

The first term in this expression is minus the sampled-and-held copies of the modulating waveform $f(t)$. This cancels out when taking the case $m = 0$ into account when calculating the total PWM output signal. The last term produces impulses in the frequency domain at integer multiples of the ω_s and since only the case where ω is not an integer multiple of ω_s is considered here, it reduces to 0. Hence only the second term remains.

Three additional terms have to be added to produce the total modulator output $P(\omega)$. These are the Fourier series expansion of the sawtooth carrier and the modulator output at integer multiples of the switching frequency given by equation (13). Finally the sampled-and-held copy of the original modulating waveform $f(t)$ at integer multiples of the switching frequency has to be considered. Since the zero-order-hold filter has zeros at every non-zero integer multiple of the switching frequency, the only contribution that remains is the Fourier transform of the original signal at $\omega = 0$. Taking all these terms into account results in the following expression for the Fourier transform of the modulator output signal:

$$P(\omega) = ST(\omega) + \begin{cases} j \frac{e^{-j\pi \frac{\omega}{\omega_s}}}{\pi \frac{\omega}{\omega_s}} \sum_{q=-\infty}^{\infty} e^{-jq\pi} \int_{-\infty}^{\infty} e^{-j\pi \frac{\omega}{\omega_s} f(t)} e^{-j(\omega-q\omega_s)t} dt & \text{if } \omega \neq 0, \pm\omega_s, \pm 2\omega_s, \dots \\ \frac{j}{m\pi} F_{em}(0) & \text{if } \omega = m\omega_s, \text{ where } m \text{ is a non-zero integer} \\ F(0) & \text{if } \omega = 0 \end{cases}$$

REFERENCES

- [1] T. Mouton and B. Putzeys, "Digital control of a PWM switching amplifier with global feedback," in *Audio Engineering Society Conference: 37th International Conference: Class D Audio Amplification*, 8 2009. [Online]. Available: <http://www.aes.org/e-lib/browse.cfm?elib=15218>
- [2] L. Risbo, "Discrete-time modeling of continuous-time pulse width modulator loops," in *Audio Engineering Society Conference: 27th International Conference: Efficient Audio Power Amplification*, 9 2005. [Online]. Available: <http://www.aes.org/e-lib/browse.cfm?elib=13263>
- [3] B. Putzeys, "Simple, ultralow distortion digital pulse width modulator," in *Audio Engineering Society Convention 120*, 5 2006. [Online]. Available: <http://www.aes.org/e-lib/browse.cfm?elib=13498>
- [4] C. Neesgaard and L. Risbo, "PWM amplifier control loops with minimum aliasing distortion," in *Audio Engineering Society Convention 120*, 5 2006. [Online]. Available: <http://www.aes.org/e-lib/browse.cfm?elib=13497>
- [5] H. Black, *Modulation Theory*. New York: von Nostrand, 1953.
- [6] D. Holmes and T. Lipo, *Pulse Width Modulation for Power Converters (Principles and Practice)*. IEEE Press Series on Power Engineering, 2003.
- [7] J. Boys and P. Handley, "Harmonic analysis of space vector modulated PWM waveforms," *Electric Power Applications, IEE Proceedings B*, vol. 137, no. 4, pp. 197 – 204, Jul. 1990.
- [8] A. Kwasinski, P. Krein, and P. Chapman, "Time domain comparison of pulse-width modulation schemes," *Power Electronics Letters, IEEE*, vol. 1, no. 3, pp. 64 – 68, 2003.
- [9] H. Deng, L. Helle, Y. Bo, and K. Larsen, "A general solution for theoretical harmonic components of carrier based PWM schemes," in *Applied Power Electronics Conference and Exposition, 2009. APEC 2009. Twenty-Fourth Annual IEEE*, 2009, pp. 1698 –1703.
- [10] B. McGrath, D. Holmes, and T. Lipo, "Optimized space vector switching sequences for multilevel inverters," *Power Electronics, IEEE Transactions on*, vol. 18, no. 6, pp. 1293 – 1301, 2003.
- [11] W. Lau, B. Zhou, and H. Chung, "Compact analytical solutions for determining the spectral characteristics of multicarrier-based multilevel PWM," *Circuits and Systems I: Regular Papers, IEEE Transactions on*, vol. 51, no. 8, pp. 1577 – 1585, 2004.
- [12] A. Lewicki, Z. Krzeminski, and H. Abu-Rub, "Space-vector pulselwidth modulation for three-level npc converter with the neutral point voltage control," *Industrial Electronics, IEEE Transactions on*, vol. 58, no. 11, pp. 5076 – 5086, nov. 2011.
- [13] D. Holmes, "A general analytical method for determining the theoretical harmonic components of carrier based PWM strategies," in *Industry Applications Conference, 1998. Thirty-Third IAS Annual Meeting. The 1998 IEEE*, vol. 2, 1998, pp. 1207 – 1214.
- [14] J. A. Houldsworth and D. A. Grant, "The use of harmonic distortion to increase the output voltage of a three-phase PWM inverter," *Industry Applications, IEEE Transactions on*, vol. IA-20, no. 5, pp. 1224 –1228, 1984.
- [15] I. Deslauriers, N. Avdiu, and B. T. Ooi, "Naturally sampled triangle carrier PWM bandwidth limit and output spectrum," *Power Electronics, IEEE Transactions on*, vol. 20, no. 1, pp. 100 – 106, 2005.
- [16] T. Barton, "Pulse-width modulation waveform – the bessel approximation," in *IEEE Industry Applications Society Annual meeting*, 1978, pp. 1125 – 1130.
- [17] R. Guinee and C. Lyden, "A novel Fourier series time function for modeling and simulation of PWM," *Circuits and Systems I: Regular Papers, IEEE Transactions on*, vol. 52, no. 11, pp. 2427 – 2435, 2005.
- [18] ———, "A single Fourier series technique for the simulation and analysis of asynchronous pulse width modulation in motor drive systems," in *Circuits and Systems, 1998. ISCAS '98. Proceedings of the 1998 IEEE International Symposium on*, vol. 6, 1998, pp. 653 – 656.
- [19] M. Mirkazemi-Moud, B. Williams, and T. Green, "A novel simulation technique for the analysis of digital asynchronous pulse width modulation," *Industry Applications, IEEE Transactions on*, vol. 30, no. 5, pp. 1284 – 1289, 1994.
- [20] G. Watson, *Theory of Bessel Functions*. Cambridge University Press, 1944.
- [21] M. Odavic, M. Sumner, P. Zanchetta, and J. Clare, "A theoretical analysis of the harmonic content of pwm waveforms for multiple-frequency modulators," *Power Electronics, IEEE Transactions on*, vol. 25, no. 1, pp. 131 – 141, Jan. 2010.
- [22] J. Carson, "Notes on the theory of modulation," *Proc. IRE*, vol. 10, pp. 57 – 64, 1922.
- [23] A. Oppenheim, W. Schafer, and J. Buck, *Discrete-time signal processing*. Prentice Hall, 1998.